Modeling and Cascade PID Controller Design of a Spinbath Circulation Process

Immanuel R. Santjoko, Tua A. Tamba*, and Ali Sadiyoko
Department of Electrical Engineering
Parahyangan Catholic University
Bandung, Indonesia
**Corresponding author*: ttamba@unpar.ac.id

***Abstract*—This paper reports the development of a cascade PID type control scheme for a MIMO spinbath circulation process regulation. In the proposed scheme, the dynamic model of the complete spinbath circulation process is first developed using concepts from fluid dynamics. Reduction of the obtained model through lumping of identical processes as well as linearization techniques is then conducted to obtain a simplified MIMO linear system with cascading control structure. A cascade PI control configuration is then constructed to achieve simultaneous control objectives in the interacting process variables of the developed simplified model. More specifically, the proposed cascade controller is of the type of summed setpoint cascade PI that is selected for its cost-effectiveness and computational efficiency. It combines a summed setpoints to simultaneously manages multiple inputs as well as cascades of faster inner disturbance rejection to allow for the minimization of the overall process' output deviations. Simulation results for constant as well as changing setpoints are then presented to demonstrate the effectiveness of the proposed modeling and cascade control schemes.**

***Index Terms*—Spinbath Circulation, Fluid Dynamics, Cascade PID Control**

I. Introduction

The spinbath circulation is a process that is often used in the production of viscose staple fiber (VSF). The VSF itself is a synthetic fiber derived from regenerated cellulose and is typically made from wood pulp [1]. In VSF production process, the viscose solution is sprayed through a spinneret into the spinbath solution inside a spinning machine. As a result, the cellulose in the viscose solution coagulates to form filaments and other chemicals such as water, H_2S, and CS_2 [2]. Over time, the returned spinbath solution often gets diluted and contaminated, thereby necessarily require some filtration and evaporation processes [3]. The recovery of the spinbath solution and its recirculation back to the spinning machine occur in the spinbath circulation system. The design of suitable control systems to maintain appropriate operation of such a spinbath circulation process is thus necessary to ensure continuos production of high quality VSF.

The main control loop in conventional spinbath circulation proceses is characterized by a multi-input multi-output (MIMO) system. Specifically, two types of actuator groups namely pumps and control valves are used to couply regulate both the fluid level of a head tank and the fluid flow to evaporators [3]. In industrial practice, this control loop is often handled using a distributed control system (DCS). For simplicity and ease of implementation, such a DCS is often configured to implement standar decoupling method for MIMO systems whereby one of the actuator groups (i.e. control valves) is kept constant such that only the remaining actuator groups (i.e. pumps) that needs to be controlled [4]. Such a decoupling practice, however, is very conservative as it has the potential to reduce output productivity/quality, increase process' sensitivity to disturbances, as well as cause significant degradation on instruments' performance/lifetime. These thus suggest that alternative control methods for handling interacting control loops in MIMO spinbath circulation process are needed.

This paper reports the development of a cascade PID control scheme for a MIMO spinbath circulation process regulation. In the proposed scheme, the dynamic model of the complete spinbath circulation process is first developed using concepts from fluid dynamics. Reduction of the obtained model through lumping of identical processes as well as linearization techniques is then conducted to obtain a simplified MIMO linear system with cascading control structure [5]. A cascade PID control configuration is then constructed to achieve simultaneous control objectives in the interacting process variables of the developed simplified model. More specifically, the proposed cascade controller is of the type of summed setpoint cascade PID that is selected for its cost-effectiveness and computational efficiency [6], [7]. It combines a summed setpoints to simultaneously manages multiple inputs as well as cascades of faster inner disturbance rejection that reduce the overall process' output deviations [8], [9]. Simulation results show the good performance of the proposed controller for setpoint regulation and disturbance rejection purposes.

The remainder of this paper is structured as follows. System configuration and problem formulation are discussed in section III. Section III briefly describes the spinbath circulation process and then derives its complete and simplified dynamic models. Cascade control schemes are then proposed in section IV and their performances are evaluation through simulations section V. Section VI concludes the paper with final remarks.

II. System Description and Problem Formulation

A. Spinbath Circulation Process

The primary objective of the spinbath circulation process is to prepare the production material called spinbath solution

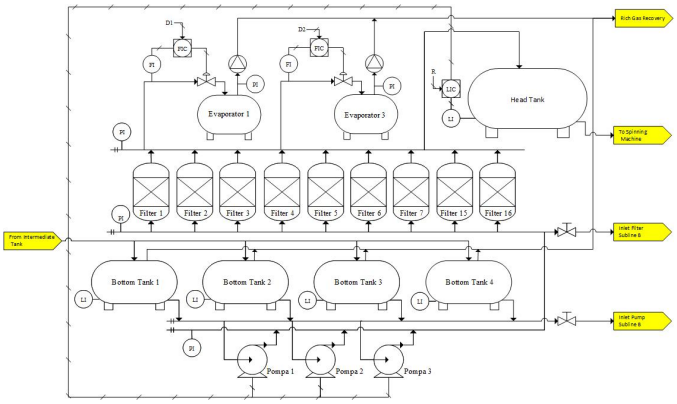

Fig. 1. P&ID schematic of the spinbath circulation process.

with appropriate concentration for *Cellulose Xanthate* regeneration process in the spinning machine. In addition, it is also used to ensure that such materials are in proper condition to be reused in the subsequent spinning processes. With regard to the latter objective, it is strictly required that the flow of the processed material to the subsequent spinning machine to be stable to maintain the high quality of the output products.

Fig. 1 shows the process and instrument diagram (P&ID) schematic of the spinbath circulation process considered in this paper. The bottom tank serves as a buffer tank and acts as a control volume to maintain the spinbath volume in the circulation system. The return spinbath solution contains various impurities which includes residues, contaminants, and carried tow. As a consequence, this spinbath solution needs to be pumped through a group of parallel filters. A portion of the filtered spinbath flow is then directed to a group of evaporators that are regulated by dedicated control valves, while the remaining flows are directed to a head tank. From the head tank, the spinbath solution will flow towards the spinning machine with the help of gravitational force. Throughout this process, it is required that both the input flow to evaporators and the fluid level on the head tank remain stable.

Based on the previously described spinbath circulation process, two types of involved control variables are proposed to be used. The first one is the input flow to the evaporator which is required to remain constant with small tolerable deviation to ensure proper operation of the evaporator. The value of this input flow is determined by both the main pumps as well as control valve attached to each evaporator's input pipe. The second control variable is the fluid level on the head tank which should be maintained on a constant level value to prevent fluctuations of the fluid flowing to the spinning machine and thereby ensure the high quality of the produced VSF outputs. This fluid level of the head tank is determined by both the main pumps as well as the amount of fluid flowing to evaporators. The presence of these two interacting control variables thus define the MIMO characteristic of the spinbath circulation process.

B. Simplified Spinbath Circulation Scheme

For the purpose of analysis and design tractability, this paper considers a simplified configuration of the spinbath circulation process as described in section II-A. This consideration is motivated by the observation that some of the involved units/instruments in the process are identical and therefore can be lumped into a single representative unit/instrument without a significant loss of generality. In this regard, each group of the bottom tanks, main pumps, and filters in the process will be lumped together and then represented as a single unit of bottom tank, main pump, and filter, respectively. To develop the model, using fluid dynamics, the steady-state equations are derived and then linearized, assuming the system dynamics are of first order. This modeling approach relies on estimated system parameters and dynamics. Several assumptions are made, including that the fluid is incompressible, the system is time-invariant, and there are no delays, among other assumptions that will be specified later. The schematic of the simplified system is illustrated in Fig. 2.

There are eight inspection points, each with the following fluid characteristics: pressure (p), density (ρ), gravitational acceleration (g), velocity (V), and elevation gain (z). The system includes 3 actuators: two control valves with evaporator 1 valve opening (L_5) and evaporator three valve openings (L_6), and one pump with angular speed (ω). There are 3 outputs: head tank level (Y), evaporator 1 flow rate (Q_5), and evaporator 3 flow rate (Q_6) which can be obtained from the product of velocity and cross-sectional area ($V \cdot A$), where (A) is the cross-sectional area of the channel.

C. Problem Formulation

The pump's angular speed directly affects both the evaporator flow and the head tank level, while the control valve directly affects the evaporator flow and indirectly affects the head tank level. Currently, there are three control loops

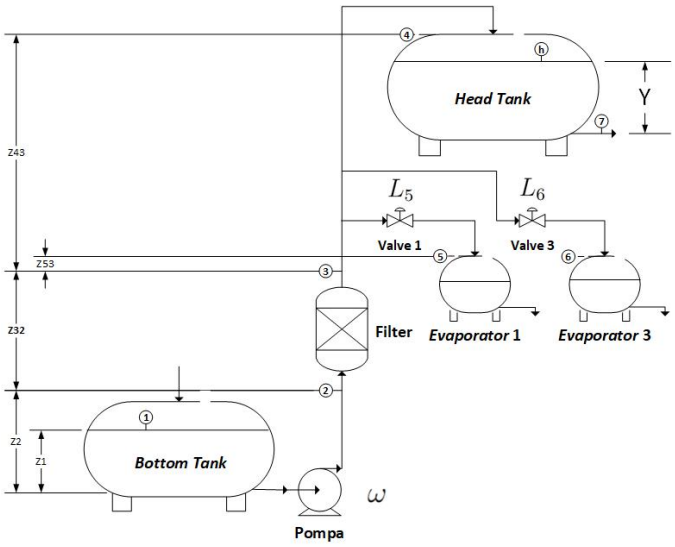

Fig. 2. Schematic of the simplified spinbath circulation process.

that are not interconnected to each other: one single-loop to regulate the head tank level and two single-loop to regulate the evaporator flow. Thus, changes in the evaporator flow setpoint are viewed as a disturbance to the head tank inlet flow. This causes deviations in the head tank level, which then translate to deviations in the spinning machine flow rate, ultimately resulting in poor product quality.

III. System Modelling

Based on the simplified system schematic in Fig. 2, the model derivation is divided into several sections according to the main components of the system, namely: pump, filter, head tank flow, head tank level, evaporator 1, and evaporator 3. Each component is analyzed independently based on fluid dynamics concept and taking into account the friction head parameter (h_f) with k as a resistance constant.

A. Pump

The pump head (h_p) can be approximated using the following two-dimensional equation [10]

$$h_p = A\omega^2 + B\omega Q - CQ^2 \tag{1}$$

where A, B, and C are pump head constants. From inspection point 1 and 2, the pressure at the bottom of the tank is known to be zero ($P_1 = 0$) as it is exposed to the atmospheric pressure. Additionally, the velocity at the bottom of the tank can be assumed to be negligible ($V_1 \approx 0$) because the large size of the tank area renders changes in velocity insignificant. Based on such a steady flow energy assumption [11], the head of the pump system can be calculated as in (2).

$$\begin{aligned} \cancel{\frac{p_1}{\rho g}}^{0} + \cancel{\frac{V_1^2}{2g}}^{0} + z_1 &= \frac{p_2}{\rho g} + \frac{V_2^2}{2g} + z_2 - h_p + h_{f2} \\ h_P &= \frac{p_2}{\rho g} + z_{21} + \left(\frac{1}{2{A_2}^2 g} + k_2\right) Q^2 \end{aligned} \tag{2}$$

By combining (1) and (2), the equilibrium point $f_1(p_2, \omega, Q)$ formula in (3) can be obtained.

$$\begin{aligned} A\omega^2 + B\omega Q + CQ^2 &= \frac{p_2}{\rho g} + z_{21} + \left(\frac{1}{2{A_2}^2 g} + k_2\right) Q^2 \\ f_1(p_2, \omega, Q) &= \frac{p_2}{\rho g} - A\omega^2 - B\omega Q \\ &\quad + \left(C + \frac{1}{2{A_2}^2 g} + k_2\right) Q^2 \end{aligned} \tag{3}$$

Assuming (1,1,1) to be the equilibrium point f_1, the linearized dynamics which ignores higher order terms around such an equilibrium can be obtained using linearization method and is given as follows.

$$f_1(p_2, \omega, Q) = c_1 \Delta p_2 - c_2 \Delta\omega + c_3 \Delta Q \tag{4}$$

where $c_1 = 1/\rho g$, $c_2 = 2A{+}1$, and $c_3 = B{+}2C{+}2/(2{A_2}^2 g)$. Assuming further that the transient response of the model is of first-order type, the constant c_2/c_1 can be represented as atransfer function G_1 while c_3/c_1 can be represented as another transfer function G_2. Specifically, G_1 is assumed to be of the form $\alpha_1/(\tau_1 s + \beta_1)$ and G_2 by $\alpha_2/(\tau_2 s + \beta_2)$. Therefore, the model of the pump can be written as follows.

$$\Delta p_2 = G_1 \Delta\omega - G_2 \Delta Q \tag{5}$$

In this paper we assume $\alpha_1 = \beta_1 = \beta_2 = \tau_1 = \tau_2 = 1$ while $\alpha_2 = 0.2$ for simplicity.

B. Filter

From inspection points 2 and 3, the inlet velocity (V_2) and the outlet velocity (V_3) of the filter are assumed to be the same, thereby can be cancelled out in the energy balance. Using steady flow energy equation [11], the head of the filter system equilibrium $f_2(p_2, p_3, Q)$ satisfies the equation below.

$$\begin{aligned} \frac{p_2}{\rho g} + \cancel{\frac{V_2^2}{2g}}^{0} + z_2 &= \frac{p_3}{\rho g} + \cancel{\frac{V_3^2}{2g}}^{0} + z_3 + h_{f3} \\ f_2(p_2, p_3, Q) &= -\frac{p_2}{\rho g} + \frac{p_3}{\rho g} + z_{32} + k_3 Q^2 \end{aligned} \tag{6}$$

Again, by assuming (1,1,1) to be the equilibrium point f_2, the linearized dynamics around this equilibrium can also be expressed as follows [12].

$$f_2(p_2, p_3, Q) = -c_4 \Delta p_2 + c_5 \Delta p_3 + c_6 \Delta Q \tag{7}$$

By further assuming that the transient response of the model is of first-order type, the constant c_{10}/c_9 can be represented as a transfer function G_7. Specifically, G_3 is given by $\alpha_3/(\tau_3 s + \beta_3)$ and G_4 by $\alpha_4/(\tau_4 s + \beta_4)$. Thus, the filter model can be written as (8) in which $c_4 = 1/\rho g$, $c_5 = 1/\rho g$, and $c_6 = 2k_3$.

$$\Delta p_3 = G_3 \Delta p_2 - G_4 \Delta Q \tag{8}$$

Here, we assume $\alpha_3 = \beta_3 = \beta_4 = \tau_3 = \tau_4 = 1$ while $\alpha_4 = 0.2$ for simplicity.

C. Head Tank Flow

Using law of mass conservation, the total mass flow rate into the system $\Sigma \dot{m}_i$ equals the total mass flow rate out of the system $\Sigma \dot{m}_o$. Assuming that the fluids are incompressible, the relationships in (9) can be obtained.

$$\begin{aligned} \dot{m}_3 &= \dot{m}_4 + \dot{m}_5 + \dot{m}_6 \\ \rho Q_3 &= \rho_4 Q_4 + \rho_5 Q_5 + \rho_6 Q_6 \\ Q &= Q_4 + Q_5 + Q_6 \end{aligned} \tag{9}$$

From inspection points 3 and 4, the pressure in the head tank is assumed to be zero ($p_4 = 0$) because it is exposed to the atmospheric pressure. Furthermore, the inlet velocity of the head tank (V_4) is assumed to be equal to the outlet velocity of the filter (V_3). This means that they cancel each other out. Based on steady flow energy equation [11], the equilibrium $f_3(p_3, Q_4)$ of the head tank flow system satisfies the following.

$$\begin{aligned} \frac{p_3}{\rho g} + \cancel{\frac{V_3^2}{2g}}^{0} + z_3 &= \cancel{\frac{p_4}{\rho g}}^{0} + \cancel{\frac{V_4^2}{2g}}^{0} + z_4 + h_{f4} \\ f_3(p_3, Q_4) &= -\frac{p_3}{\rho g} + z_{43} + k_4 {Q_4}^2 \end{aligned} \tag{10}$$

Assuming (1,1) to be the equilibrium f_3, the linearized dynamics around this equilibrium can be expressed as follows.

$$f_3(p_3, Q_4) = c_7 \Delta p_3 + c_8 \Delta Q_4 \tag{11}$$

where $c_7 = 1/\rho g$ and $c_8 = 2k_4$. Assuming that the transient response of the model is of first-order type, the constant c_8/c_7 can be represented as a transfer function $G_5 = \alpha_5/(\tau_5 s + \beta_1)$. Therefore, the head tank flow model can be written as

$$\Delta Q_4 = G_5 \Delta p_3 \tag{12}$$

where $\alpha_5 = \tau_5 = \beta_5 = 1$ are assumed.

D. Head Tank Level

Assuming mass conservation [11], the change of mass in the head tank ($\dot{m}_h$) is influenced by the mass entering the head tank ($\dot{m}_4$) minus the mass leaving the head tank ($\dot{m}_7$). If the mass leaving the head tank ($\dot{m}_7$) is constant, the head tank level can be modeled as follows.

$$\begin{aligned} \frac{dm}{dt} &= \dot{m}_4 - \dot{m}_7 \\ \rho A \frac{dy}{dt} &= \rho(Q_4 - Q_7) \\ Y(s) &= (Q_4(s) - Q_7(s))\, G_6 \end{aligned} \tag{13}$$

with $G_6 = \alpha_{10}/\tau_{10} s$ with $\alpha_{10} = 1$ and $\tau_{10} = 10$ are assumed. The pressures in the head tank and the spinning machine are zero ($p_4 = p_7 = 0$) because they are open to and have direct contact with the atmospheric pressure. The velocity at the head tank is assumed to be negligible (V_h) because the large tank area renders the changes in level to be insignificant.

Based on steady flow energy assumption [11], the head equilibrium of the head tank level system satisfies (14).

$$\begin{aligned} \cancel{\frac{p_h}{\rho g}}^{0} + \cancel{\frac{{V_h}^2}{2g}}^{0} + z_h &= \cancel{\frac{p_7}{\rho g}}^{0} + \frac{{V_7}^2}{2g} + z_7 - h_p + h_{f7} \\ f_4(Y, Q_7) &= -Y + \left(\frac{1}{2{A_7}^2 g} + k_7 \right) {Q_7}^2 \end{aligned} \tag{14}$$

Assuming (1,1) to be the equilibrium point f_4, the linearized dynamics around this equilibrium satisfies the following.

$$f_4(Y, Q_7) = -c_9 \Delta Y + c_{10} \Delta Q_7$$

where $c_9 = 1/\rho g$ and $c_{10} = 2/(2{A_7}^2 g) + 2k_7$. By further assuming that the transient response of the model is of first-order type, the constant c_{10}/c_9 is represented as a transfer function of the form $G_7 = \alpha_7/(\tau_7 s + \beta_7)$ in which the values $\alpha_7 = \tau_7 = \beta_7 = 1$ are assumed. Therefore, the head tank level model can be written as follows.

$$\Delta Q_7 = G_7 \Delta Y \tag{15}$$

E. Evaporator

For the evaporator system, the inlet velocity (V_3) and the outlet velocity (V_5) are assumed to be the same and can be cancelled out in the energy balance equation. It is also assumed that the control valve respons is a linear function of the form ($F_{(L_5)} = 1/L_5$), the pressure within evaporator 1 (p_5) remains constant, and the pipe resistance is negligible. Based on steady flow energy equation [11], the head's equilibrium of the evaporator system satisfies the following equation.

$$\begin{aligned} \frac{p_3}{\rho g} + \frac{{V_3}^2}{2g} + z_3 &= \frac{p_5}{\rho g} + \cancel{\frac{{V_5}^2}{2g}}^{0} + z_5 + h_{f5} \\ f_5(p_3, L_5, Q_5) &= -\frac{p_3}{\rho g} + \frac{p_5}{\rho g} + z_{53} + (k_5 + F_{(L_5)}){Q_5}^2 \\ &= -\frac{p_3}{\rho g} + \frac{p_5}{\rho g} + z_{53} + \frac{1}{L_5}{Q_5}^2 \end{aligned} \tag{16}$$

Assuming (1,1,1) to be the equilibrium point f_1, the linearized dynamics around this equilibrium satisfies the following.

$$f_5(p_3, L_5, Q_5) = -c_{11} \Delta p_3 + c_{12} \Delta L_5 + c_{13} \Delta Q_5 \tag{17}$$

where $c_{11} = 1/\rho g$, $c_{12} = 1$, and $c_{13} = 2$. Further assuming that the transient response of the model is of first-order type, the constant c_{11}/c_{13} can be represented as a transfer function G_8 and c_{12}/c_{13} is represented as the transfer function G_9. Specifically, G_8 is given by $\alpha_8/(\tau_8 s + \beta_8)$ and G_9 by $\alpha_9/(\tau_9 s + \beta_9)$, respectively, where the values $\alpha_8 = \alpha_9 = \beta_8 = \beta_9 = 1$ and $\tau_8 = \tau_9 = 3$ are assumed. Thus, the evaporator 1 can be modeled as.

$$\Delta Q_5 = G_8 \Delta p_3 + G_9 \Delta L_5 \tag{18}$$

If one assumes that evaporator 3 have the same parameters as that of evaporator 1, then (19) can be obtained with $G_{10} = G_8$ and $G_{11} = G_9$.

$$\Delta Q_6 = G_{10} \Delta p_3 + G_{11} \Delta L_6 \tag{19}$$

F. System Block Diagram

Based on aforementioned modeling, the block diagram of the simplified model can be constructed as shown in Fig. 3.

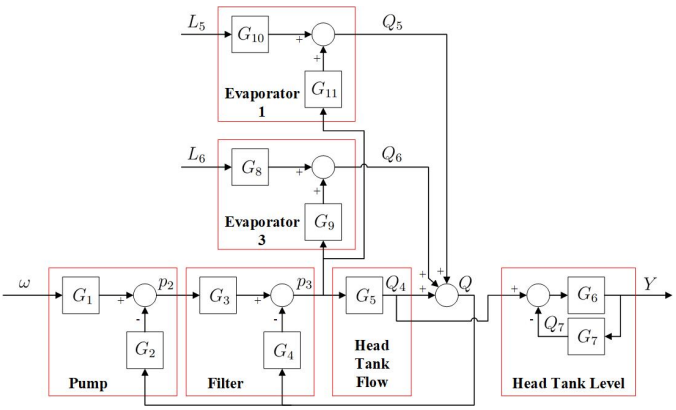

Fig. 3. Block diagram of the simplified model.

Note in this figure that the simplified model has three inputs, namely the pump's angular speed (ω), evaporator 1's valve opening (L_5), and evaporator 3's valve opening (L_6). Since the evaporator flow rates are not critical for the control objectives, the output in the simplified model is set to be head tank's level (Y). The pump's angular speed directly affects the evaporator flow and the head tank level positively, while each evaporator valve opening directly affects each corresponding evaporator's flow positively while indirectly affects other evaporators as well the head tank's level negatively through the corresponding decrease in pump and filter pressures.

IV. Control System Design

Based on the block diagram of the simplified model in Fig. 3, three control systems were developed to regulate the head tank level, namely: (i) a control system for the assumed single-loop model, (ii) a conventional cascade controller, and (iii) a summed setpoint cascade controller. We point out that other control systems such as MPC and other decoupling controller [6], [7] have also been proposed for the considered system. However, in the Yokogawa CentumVP DCS, the MPC function block is prohibitively expensive, while the calculator is limited to only 70 lines of code, making it insufficient for more complex calculations. Additionally, computer implementation of the decoupling controller is known to be highly complex and, thus, is relatively not feasible for practical implementations.

A. Single-loop Control System

For the original system structure as depicted in the P&ID schematic in Fig. 1, a multiple single-loop controller is developed. This controller includes one single-loop controller (C_1) to regulate the head tank level with R as its setpoint, and two additional single-loop controllers C_6 and C_7 to regulate the flows of evaporator 1 and evaporator 3 with setpoint values of D_1 and D_2, respectively. All controllers are PID type and the resulting closed loop block diagrams is shown in Fig. 4. The head tank level controller adjusts the pump angular speed, which directly affects both the head tank level and the evaporator flow rate positively. Since the evaporator flow rates are not critical for the control objectives, minor variations are viewed acceptable. The evaporator flow controllers adjusts valve openings, which indirectly affect the head tank level negatively. Consequently, a change in the evaporator flow

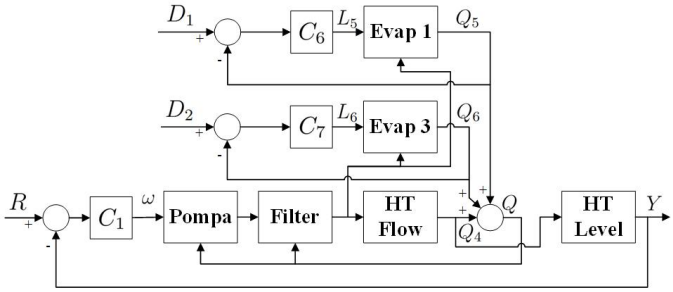

Fig. 4. Block diagram of the single-loop control system.

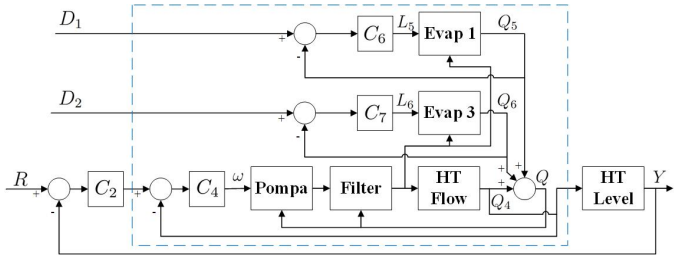

Fig. 5. Block diagram of the conventional cascade control system.

setpoint can introduce a disturbance to the head tank control loop, leading to a significant deviation in the head tank level.

B. Conventional Cascade Control System

To address the limitations of the single-loop controller, a cascade control system is proposed to regulate the head tank level. The outer loop controller (C_2) regulates the head tank level (Y) with R as a setpoint, while the inner loop controller (C_3) regulates the head tank flow rate (Q_4). All controllers utilize the PID algorithm and the resulting block diagram is shown in Fig. 5. Here, the outer loop controller adjusts the setpoint of the head tank flow, which serves as the setpoint for the inner loop controller. The inner loop controller then adjusts the pump angular speed. Note that the evaporator flow controllers still indirectly affect the head tank level negatively, acting as a disturbance to the head tank loop. However, with the inner loop controller's faster response time, the deviations in the head tank level are reduced.

C. Summed Setpoint Cascade Control System

To address the limitations of the aforementioned single-loop and conventional cascade controllers, a summed setpoint cascade control system is proposed to regulate the head tank level. The outer loop controller (C_4) regulates the head tank level (Y) with R as its setpoint, while the inner loop controller (C_5) regulates the total flow rate (Q). All controllers utilize PID algorithm and the resulting block diagram of cascade control system is illustrated in Fig. 6.

The outer loop controller adjusts the head tank flow setpoint, which then summed with the flow setpoints of evaporator 1 and 3, and used as the setpoint for the inner loop controller. The inner loop controller then adjusts the pump angular speed. By summing these setpoints, the evaporator flow controllers both directly and indirectly affect the head tank level in positive

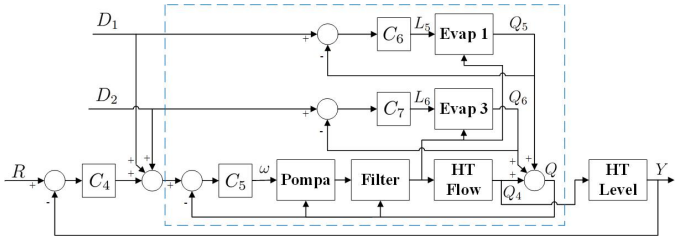

Fig. 6. Block diagram of the summed setpoint cascade control system.

TABLE I
PID PARAMETERS OF THE SYSTEMS.

Controller	System Parameter		PID Parameter		
	Response Time	Transient Behavior	K_p	K_i	K_d
C_1	20s	0.7	1.2277	0.1565	0
C_2	8s	0.7	0.9687	0.0971	0
C_3	20s	0.7	0.3224	0.3519	0
C_4	8s	0.7	0.9687	0.0971	0
C_5	20s	0.7	0.3224	0.3519	0
C_6 & C_7	3	0.7	1.2321	1.2440	0

and negative directions. The summation thus acts as a partial decoupling, leading to reduced deviation in head tank level.

V. Simulation Results

Simulations were performed in MATLAB [13] to evaluate the performace of all three control system schemes as described in section IV. In each scheme, the tuning of the PID controller parameters is performed from the innermost controller to the outermost controller [9]. In our simulations, the tuning is performed using MATLAB's PID Tuner with adjustment on the closed loop response times to achieve the best response results [14]. The selected tuning results in a robustness index of 0.7 and a response time ratio between the inner and outer controllers of 1:2.5. The resulting PID parameters as summarized in Table I suggest that a PI controller is sufficient for each control structure. In the following subsections, more detailed simulation results for each control scheme under PID controller parameter in Table I are discussed.

A. Step Response Simulation Result

Two simulations were conducted in MATLAB to analyze the step response of the control systems from simplified the spinbath circulation model in Figs. 4, 5, and 6 for inputs R and D_1. Zero initial conditions and a sampling time of $T_s = 70$s

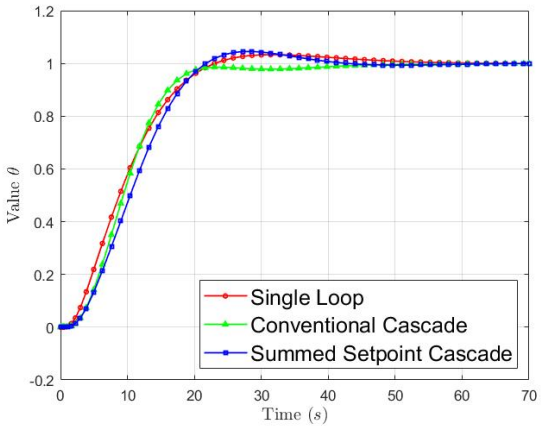

Fig. 7. Step responses of all controllers to input R.

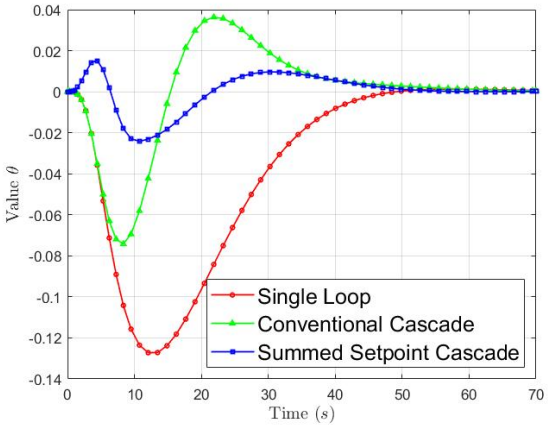

Fig. 8. Responses of all controllers to disturbance input D.

are used. Fig. 7 plots the step response of the closed loop system for all controllers for the input R, while Fig. 8 plots the response of the closed loop system to disturbance signal D. From these plots, the resulting response characteristics as well as integral absolute error (IAE) values are extracted and summarized in Table II.

Fig. 7 shows that all three control schemes have closely similar step response characteristics to input R. The responses in this figure also reveal that the peak value and integral absolute error (IAE) differ only slightly among the three control schemes. All control schemes exhibit overshoots within tolerable values of less than 10%, with the conventional cascade control system demonstrating slightly superior performance in terms of rise time and settling time criteria.

For the response to disturbance input D in Fig. 8, the conventional and summed setpoint cascade control system however show better performance as compared to that of the single-loop control system in term of minimizing the response deviation. This thus suggest that cascade controllers significantly outperform the single-loop controller in terms of disturbance rejection capability. Specifically, the peak value in the summed setpoint cascade control system is reduced by approximately 81%, indicating a much smaller deviation from the desired output in the presence of disturbances. Additionally, the integral absolute error (IAE) for the summed setpoint cascade control system is reduced by 83%, highlight-

TABLE II
STEP RESPONSES AND IAE OF DIFFERENT CONTROL STRUCTURES

Information	single-loop		Conv. Cascade		S.S. Cascade	
	R	D	R	D	R	D
Rise Time	13.90	-	11.80	-	13.35	-
Settling Time	35.16	20.38	20.06	44.28	26.32	36.74
Peak Max	1.033	0.001	1	0.036	1.045	0.015
Peak Min	-	-0.127	-	-0.074	-	-0.024
IAE	10.24	2.599	10.30	1.153	11.40	0.443

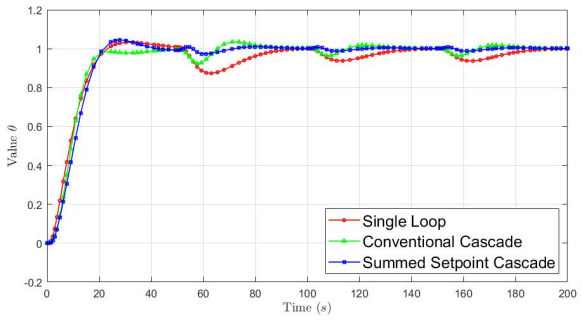

(a)

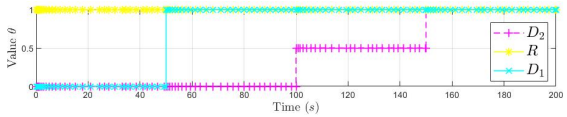

(b)

Fig. 9. System response for changing setpoints: (a) response, (b) setpoint.

ing a substantial improvement in maintaining adherence to the setpoint over time. While the conventional cascade control system also shows improvements by reducing both the peak value and IAE, the summed setpoint cascade control system surpasses it in overall performance.

B. Multiple-Input Simulation Result

In real-world scenarios, setpoint changes often occur simultaneously. Therefore, evaluation for multiple inputs' case were also conducted to comprehensively evaluate the system performance. The simulation were conducted with zero initial condition and a sampling time of $T_s = 200$s. The inputs were set to be step functions that are delayed up to times $T = 0$ for input R and $T = 50$ for input D_1, as well as two successive 0.5 increment step functions that are delayed up to times $T = 100$ and $T = 150$, respectively, for input D_2.

Fig. 9(a) plots the closed loop system responses for all control schemes with respect to series of changing values of the setpoints shown in Fig. 9(b). It can be seen in these figures that all schemes produce similar closed loop responses. Moreover, the system characteristics remain similar to those observed in the case of single step input responses. The IAE value is 15.34 for the case of using single-loop controller, 12.55 for the case of using conventional cascade controller, and 12.28 for the case of using the summed setpoint cascade controller. These thus indicate the better performance of the summed setpoint controller In real-life applications, there is often a tolerable maximum deviation value, and changes in the evaporator flow setpoint occur much more frequently than changes in the head tank level setpoint. This means that the summed setpoint can be achieved in a larger time steps whereas the single-loop controller must be broken down into many smaller step responses.

VI. Conclusion

This paper has presented the modeling and cascade controller design of a MIMO spinbath circulation process. The model is constructed using concepts from fluid dynamics while the cascade control scheme is designed using the summed setpoint cascade PI structure. Simulation results for constant and changing sepoint values are also reported to demonstrate the effectiveness of the proposed modeling and control schemes.

References

[1] J. Chen, "Synthetic textile fibers: Regenerated cellulose fibers," in *Textiles and Fashion (Ch. 4)*, ser. Woodhead Publishing Series in Textiles, R. Sinclair, Ed. Woodhead Publishing, 2015, pp. 79–95.

[2] I. S. Mendes, A. Prates, and D. V. Evtuguin, "Production of rayon fibres from cellulosic pulps: State of the art and current developments," *Carbohydrate Polymers*, vol. 273, p. 118466, 2021.

[3] APR, *Asia Pacific Rayon: Process and Technical Description Modules*, Asia Fibre Trading Pte Ltd, Accessed on: 2020.

[4] A. Reyes-Lúa and S. Skogestad, "Multiple-input single-output control for extending the steady-state operating range—use of controllers with different setpoints," *Processes*, vol. 7, no. 12, 2019.

[5] R. B. Sartor, J. O. Trierweiler, and P. R. B. Fernandes, "Obtaining linearized dynamic models from steady-state simulations," in *Seminario do Programa de Pos-Graduacao em Engenharia Quimica (10.: 2011 out. 04-07: Porto Alegre, RS)*, 2011, pp. 1–6.

[6] R. Nian, J. Liu, and B. Huang, "A review on reinforcement learning: Introduction and applications in industrial process control," *Computers & Chemical Engineering*, vol. 139, p. 106886, 2020.

[7] L. Liu, S. Tian, D. Xue, T. Zhang, Y. Chen, and S. Zhang, "A review of industrial mimo decoupling control," *International Journal of Control, Automation and Systems*, vol. 17, no. 5, pp. 1246–1254, 2019.

[8] A. Celna *et al.*, "Centralized frequency control of offshore hybrid power plant," in *Proc. 8th International Hybrid Power Plants & Systems Workshop*, 2024, pp. 106–114.

[9] R. Vilanova and O. Arrieta, "PID tuning for cascade control system design," in *Proc. Canadian Conference on Electrical and Computer Engineering*, 2008, pp. 001 775–001 778.

[10] G. Janevska, "Mathematical modeling of pump system," in *Electronic International Interdisciplinary Conf.*, vol. 2, 09 2013, pp. 455–458.

[11] F. White, *Fluid Mechanics*. McGraw-Hill Education, 2015.

[12] K. Ogata, *Modern Control Engineering*. Prentice Hall, 2010.

[13] MATLAB, *ver. R2020a*. Natick, MA, USA: The MathWorks Inc., 2020.

[14] L. Wang, *PID control system design and automatic tuning using MATLAB/Simulink*. John Wiley & Sons, 2020.